Direct modal transition from space wave to surface wave leakage on microstrip lines

P. Baccarelli,[1] P. Burghignoli,[1] G. Lovat,[2] S. Paulotto,[1] F. Mesa,[3] and D. R. Jackson[4]

Received 12 May 2005; revised 30 August 2005; accepted 28 September 2005; published 31 December 2005.

[1] In this paper it is shown for the first time that a novel transition may occur for dominant (quasi transverse electromagnetic (quasi-TEM)) leaky modes on microstrip line, between a leaky mode that leaks into the TM_0 surface wave mode and one that leaks both into the surface wave and into space. The modal evolution of leaky modes as a function of frequency is studied by means of a full-wave spectral domain approach, and it is shown that such transitions occur on microstrip lines that have a critical strip width, which is relatively large. When the strip width is equal to the critical value, a transition frequency will exist at which the attenuation constant of the leaky mode drops exactly to zero and the leaky mode has a real propagation wave number exactly equal to the free-space wave number. At this frequency, the leaky mode transitions from one that leaks into only the surface wave to one that also leaks into space. In a frequency neighborhood of the transition frequency, very large spurious effects may be produced because of interference between the fundamental quasi-TEM mode and the continuous spectrum current.

Citation: Baccarelli, P., P. Burghignoli, G. Lovat, S. Paulotto, F. Mesa, and D. R. Jackson (2005), Direct modal transition from space wave to surface wave leakage on microstrip lines, *Radio Sci.*, *40*, RS6017, doi:10.1029/2005RS003286.

1. Introduction

[2] The study of leaky modes on printed-circuit lines has received considerable attention in recent years, because of their role in the representation and explanation of spurious transmission effects [see, e.g., *Shigesawa et al.*, 1988; *Freire et al.*, 1999; *Langston et al.*, 2001; *Mesa et al.*, 2001; *Mesa and Jackson*, 2002a]. Such undesirable effects include power loss, spurious transmission dips due to interference between the fundamental quasi transverse electromagnetic (quasi-TEM) bound mode current and the leaky mode current, and crosstalk with adjacent lines or circuits.

[3] As is known, two types of leaky modes may generally exist on printed-circuit lines, that is, surface wave leaky modes (SFWLM) and space wave leaky modes (SPWLM). The former radiate while propagating along the line into one or more surface waves supported by the background planar structure; the latter, which may exist on vertically unshielded structures only, radiate both into surface waves and directly into space [*Oliner*, 1987; *Das and Pozar*, 1991; *Bagby et al.*, 1993].

[4] Until now, it has never been observed that one type of leaky mode may transition into the other type for the quasi-TEM mode on microstrip line, and in fact, such a transition was not even thought possible [*Mesa et al.*, 2002]. (Transitions from real improper modes to SPWLMs were reported by *Rodríguez-Berral et al.* [2004] for microstrip lines with an upper dielectric half-space.) It is shown here for the first time that under certain conditions, such a transition will occur. The required condition is a critical strip width, the value of which depends on the substrate permittivity and thickness. The critical strip width is fairly wide (as shown later, a strip width of about three times the substrate thickness is typical). For this critical strip width there will exist a transition frequency where one type of leaky mode transitions into the other type. At the transition frequency, the attenuation constant of the leaky modes drops exactly to zero.

[5] In addition to being an interesting new phenomenon, this discovery has practical significance as well. It is demonstrated here that severe spurious effects may be

[1]Department of Electronic Engineering, "La Sapienza" University of Rome, Rome, Italy.
[2]Department of Electrical Engineering, "La Sapienza" University of Rome, Rome, Italy.
[3]Department of Applied Physics 1, University of Seville, Seville, Spain.
[4]Department of Electrical and Computer Engineering, University of Houston, Houston, Texas, USA.

0048-6604/05/2005RS003286$11.00

observed in the current that is excited by a practical source when operating near the transition frequency, due to the extremely large continuous spectrum (CS) current that interferes with the bound mode (BM) current. The nature of the CS current near the transition frequency is explored here, and it is shown that the CS current is dominated by a leaky mode (LM) current for frequencies that are near, but not too near, to the transition frequency. Significant spurious effects then occur because of the low attenuation constant of the leaky mode [*Mesa and Jackson*, 2002a]. When the frequency is extremely close to the transition frequency, it is shown that the CS current is dominated by a "residual wave" (RW) current [*Mesa et al.*, 2001], and this current is then responsible for the spurious effects.

[6] The geometry assumed here is a microstrip line with strip width w, on a grounded dielectric slab of thickness h and relative permittivity ϵ_r. The strip conductor is assumed to be infinitesimally thin and perfectly conducting, and the substrate is assumed to be lossless in all of the results. The axis of the strip is assumed to be the z axis, and the x direction is along the interface, perpendicular to the strip. For the case of a source excitation, a 1 V gap voltage source is placed on the line at $z = 0$.

2. Background

[7] In order to calculate numerically the complex propagation constant and the modal current of a given mode with the method of moments in the spectral domain, it is necessary to adopt a particular integration path in the complex plane of the transverse spectral variable k_x, depending on the type of mode being sought (BM, SFWLM, SPWLM) [*Mesa et al.*, 1999]. The three possible paths corresponding to modal solutions that may yield physical solutions are shown in Figure 1a. The real axis path, called $\mathcal{C}_0$, is used to find the (real) wave number of the bound mode, which is always physical. The path $\mathcal{C}_1$ detours around the TM_0 poles of the layered-media Green's function, and is used to find the wave number of the SFWLM solution. This solution will be physical when the phase constant of the mode is greater than k_0 and less than k_{TM_0} [*Mesa et al.*, 1999]. The path $\mathcal{C}_2$ detours around the TM_0 poles and lies partially on the bottom Riemann sheet of the k_x plane. The corresponding SPWLM solution will be physical provided the phase constant of the mode is less than k_0 [*Mesa et al.*, 1999].

[8] The fact that different paths of integration in the k_x plane may be used for each value of k_z leads to the existence of branch points in the complex k_z plane [*Chang and Kuester*, 1979; *Grimm and Nyquist*, 1993]. A convenient tool to aid in the discussion of the paths is the concept of a Riemann surface for the longitudinal

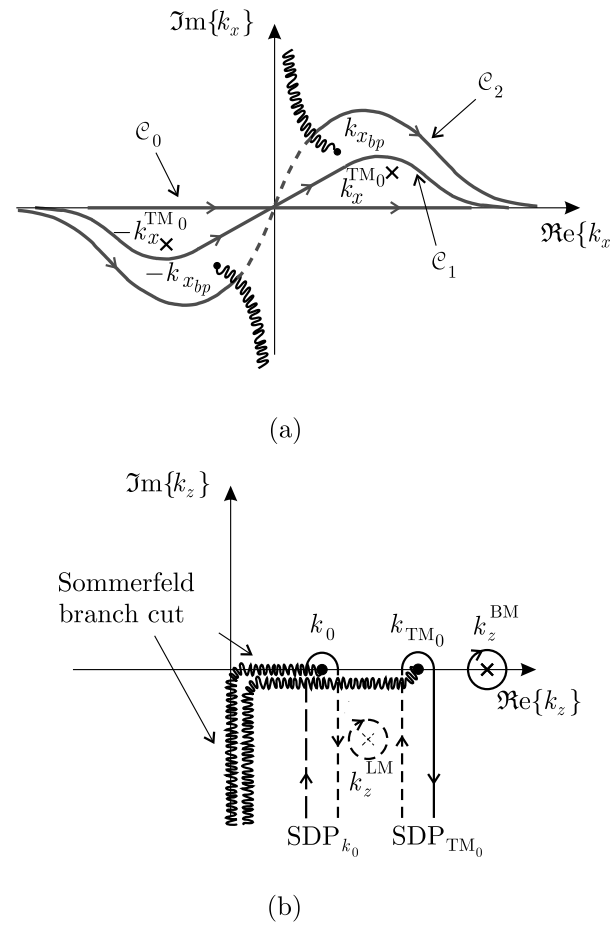

Figure 1. Spectral complex planes for an unshielded microstrip line. (a) Complex plane of the transverse spectral variable k_x, with three integration paths shown that give rise to different modal solutions. (b) Complex plane of the longitudinal spectral variable k_z, showing the k_0 and k_{TM_0} branch points (and associated Sommerfeld branch cuts), a bound mode pole k_z^{BM}, and a leaky wave pole k_z^{LM}.

wave number k_z. On this surface, each sheet corresponds to a different path of integration in the k_x plane for a given value of k_z. As first shown by *Mesa et al.* [1999], for an unshielded microstrip line, there are two different types of branch point singularities in the complex k_z plane: logarithmic-type branch points (where an infinite number of sheets merge) at $k_z = \pm k_0$ and algebraic-type branch points (where two sheets merge) at $k_z = \pm k_{bn}$, where k_0 is the free-space wave number and k_{bn} are the wave numbers of the background structure modes. (In Figure 1b it is assumed that the only background mode above cutoff is the TM_0 mode; hence there are two pairs of branch points, one at $k_z = \pm k_0$ and one at $k_z = \pm k_{TM_0}$.)

[9] A convenient method for studying the importance of leaky modes and the continuous spectrum on lines that are excited by practical sources is the gap voltage source excitation, as introduced by *Di Nallo et al.* [1998]. A 1 V gap source is assumed to excite an infinite line at $z = 0$. The resulting current on the line is expressed via an inverse Fourier transform as

$$I(z) = \frac{1}{2\pi} \int_{-\infty}^{\infty} \tilde{I}(k_z) \mathrm{e}^{-jk_z z} \mathrm{d}k_z, \tag{1}$$

where the Fourier transform of the strip current, $\tilde{I}(k_z)$, can be calculated in closed form for narrow strips (assuming that a single basis function describes the transverse variation of the current on the strip), and using a small matrix equation for wider strips, where multiple basis functions are used [*Mesa et al.*, 2001]. The integration path is along a Sommerfeld path that stays below the real k_z axis for $k_z < 0$ and above the real axis for $k_z > 0$, lying on the "zero" sheet (the one that corresponds to the path $\mathcal{C}_0$ in the k_x plane). Poles in the k_z plane appear at the wave numbers of the guided modes (bound and leaky) on the infinite microstrip line.

[10] By deforming the path of integration to a path around the branch cuts in the fourth quadrant, the total strip current can be decomposed into a BM current (which is the current of the desired quasi-TEM microstrip mode) along with a CS current that physically corresponds to a radiating type of current, which typically becomes stronger as the frequency increases. The BM current arises mathematically from the residue at the BM pole on the real axis in the k_z plane (see Figure 1b). The CS current comes from the integration around the branch cuts as shown in Figure 1b (hyberbolic, or "Sommerfeld" branch cuts are assumed in Figure 1b). The CS current may be further decomposed into a LM current and a set of two RW currents. To accomplish this, the Sommerfeld path for the total current is deformed into a residue path around the LM pole and a set of two steepest descent paths (SDPs), which are the vertical paths descending from the branch points at k_0 and k_{TM_0}. During this path deformation a LM pole will be captured if it resides on the appropriate sheet of the k_z plane, implying that the leaky mode is a physical one [*Di Nallo et al.*, 1998; *Mesa et al.*, 1999]. Using the change of variables $k_z = k_0 - js$ in (1), the k_0-RW current $I_{k_0}^{\mathrm{RW}}(z)$ has the form

$$I_{k_0}^{\mathrm{RW}}(z) = -j \frac{1}{2\pi} \int_0^{\infty} F(s)\, \mathrm{e}^{-sz}\, \mathrm{d}s, \tag{2}$$

where

$$F(s) = \tilde{I}(k_0 - js)|_R - \tilde{I}(k_0 - js)|_L, \tag{3}$$

with R denoting the right side of the SDP and L denoting the left side. A similar change of variables may be done to define the TM_0-RW current, although the focus here will be on the k_0-RW current, since this current plays a significant role in the behavior of the strip current near the transition frequency.

[11] An asymptotic analysis reveals that the k_0-RW current normally behaves for large z as [*Mesa et al.*, 2001; *Baccarelli et al.*, 2004]

$$I_{k_0}^{\mathrm{RW}} \sim A_{k_0}^{\mathrm{RW}} \frac{\mathrm{e}^{-jk_0 z}}{z^2}. \tag{4}$$

[12] Because of the fairly rapid decay, the k_0-RW current is usually not significant at great distances from the source. However, as will be demonstrated later, the k_0-RW current changes character for frequencies very close to the transition frequency, and consequently becomes both very strong in amplitude and slowly decaying.

[13] The following sections in the paper are organized as follows. In section 3 numerical examples of SFWLM-to-SPWLM transitions are given. In section 4 a physical explanation and necessary requirement for the occurrence of such a transition is given on the basis of the reciprocity theorem. Section 5 discusses the leaky mode and residual wave current excitation in a neighborhood of the transition frequency for the case of a gap voltage source. Finally, some conclusions are drawn in section 6.

3. Transition From Space Wave to Surface Wave Leakage

[14] Figure 2 shows the dispersion diagram for a microstrip line with substrate permittivity $\varepsilon_r = 10.2$, substrate thickness $h = 1$ mm, and strip width $w = 3$ mm, in a frequency range from 0 to 30 GHz. This strip width happens to be the critical strip width for this particular substrate. Three modes of the microstrip are reported: the fundamental quasi-TEM EH_0 mode (black solid line with circles), a space wave leaky mode (SPWLM) calculated with the $\mathcal{C}_2$ path in the k_x plane (gray solid line), and a surface wave leaky mode (SFWLM) calculated with the $\mathcal{C}_1$ path in the k_x plane (black solid lines). The TM_0 and TE_1 modes of the background substrate are also reported (thin dash-dotted lines).

[15] The SPWLM (gray solid line) is physical when its normalized phase constant is less than one, that is, from 19.3 to 23.29 GHz. At $f = f_t \approx 23.29$ GHz the associated pole in the k_z plane passes through the k_0 branch point, and above this frequency the SPWLM evolves into a nonphysical mode that has a negative attenuation constant. The path of integration must be changed smoothly in order to track the pole as it passes through the branch point, resulting in a nonphysical path above 23.29 GHz, which is different from either $\mathcal{C}_1$ or $\mathcal{C}_2$. This path is one

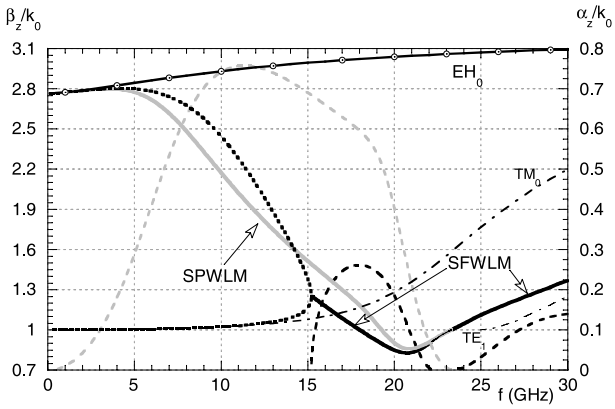

Figure 2. Normalized phase (β_z/k_0) and attenuation (α_z/k_0) constants as a function of frequency for three modes of a microstrip line with $\varepsilon_r = 10.2$, $h = 1$ mm, and $w = 3$ mm: the quasi-TEM fundamental EH_0 mode and two leaky modes (SPWLM and SFWLM). Normalized phase constant of the EH_0 mode, thick solid line with circles; normalized phase constant of the leaky modes, thick solid lines; normalized phase constants of the real improper modes, thick dotted lines; normalized attenuation constants of the leaky modes, thick dashed lines; and normalized phase constants of the TM_0 and TE_1 modes of the substrate, thin dash-dotted lines.

that would be labeled as (−1; 0; 0) in the notation of *Mesa and Jackson* [2002b]. The solution is not shown above 23.29 GHz.

[16] On the other hand, the SFWLM (black solid line) is physical when its normalized phase constant is greater than one but less than the normalized phase constant of the TM_0 mode of the substrate, that is, between 16.7 and 18 GHz and above 23.29 GHz. In the range between 22.17 and 23.29 GHz its attenuation constant (not shown here) is negative, and the mode is obtained with the nonphysical path (1; 0; 0) [*Mesa and Jackson*, 2002b].

[17] The transition from SPWLM to SFWLM can be observed in the enlarged diagram reported in Figure 3, which only shows the physical parts of the dispersion curves of the involved modes. At the transition frequency, f_t, the normalized phase constants of both modes are equal to one, while their attenuation constants are equal to zero, so that the associated poles in the complex k_z plane merge at the k_0 branch point.

[18] In order to illustrate the features of the above transition, Figure 4 shows the k_z pole trajectories corresponding to the SPWLM (gray solid line) and the SFWLM (black solid line) reported in Figure 2 for three different values of the strip width, that is, $w = 2.9$ mm, $w = w_c = 3$ mm, and $w = 3.1$ mm. The solutions corresponding to the nonphysical paths are also shown with dashed lines. It can be observed that when the strip width is equal to the critical value, w_c, both poles pass through the k_0 branch point at the transition frequency f_t, resulting in a transition from a space wave to a surface wave leaky regime.

[19] However, by changing the strip width away from the critical value, the k_z poles fail to pass through the branch point, and a direct transition no longer occurs. The SPWLW and SFWLW pole trajectories still cross, at a point slightly below the real axis in the k_z plane, but since the poles are on different sheets, they do not actually intersect on the Riemann surface. In this case, there may or may not be a spectral gap region (i.e., a frequency range where none of the two leaky modes is physical), depending on the frequencies at which the physical poles cross the vertical line $\Re e\{k_z\} = k_0$.

[20] Physical continuity between the two leaky modes is to be expected for values of the strip width in a neighborhood of the critical width. To illustrate, Figure 5 shows the transverse profile of the amplitude of the longitudinal component of the modal current as a function of the normalized transverse coordinate x/w for both the SPWLM and the SFLWM, at different frequencies below and above the transition frequency, respectively. It can be observed that the shape of the modal current is similar to that of the fundamental quasi-TEM EH_0 mode, although the current amplitude exhibits two zeros for the frequencies immediately below and above the transition frequency. Hence, very near the transition frequency, the shape of the current is more similar to that of an EH_2 mode. The curves corresponding to these two frequencies (black solid line and gray dashed line) are superimposed on the plot, verifying the expected physical continuity of the two modal solutions.

[21] Another dispersion diagram is shown in Figure 6 for a microstrip line with a lower substrate permittivity

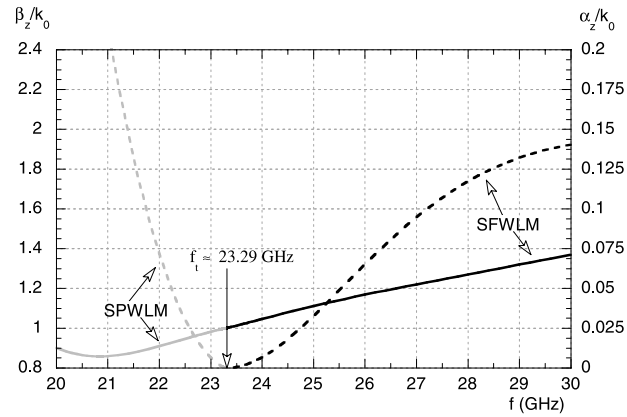

Figure 3. Enlarged plot of the dispersion curves of the SPWLM and SFWLM modes in Figure 2, in a neighborhood of the transition frequency.

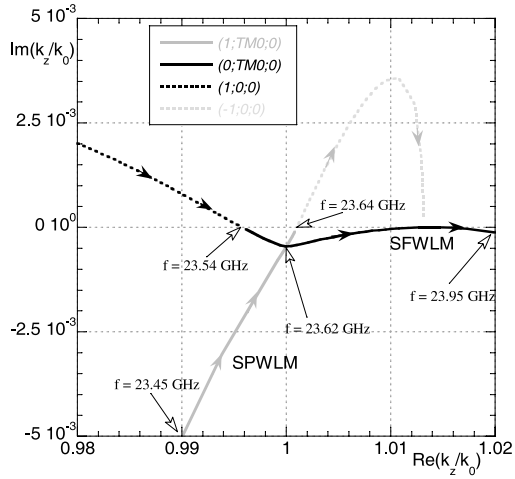

(a)

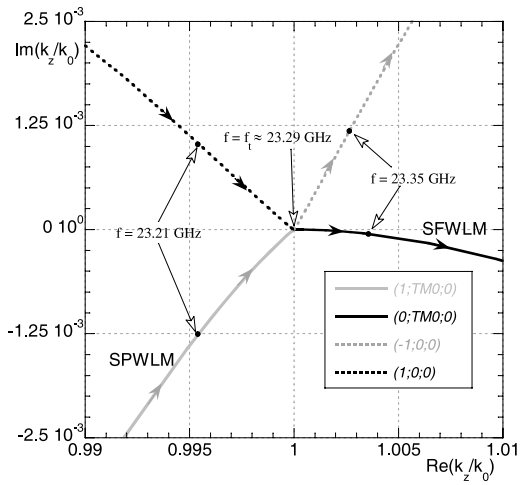

(b)

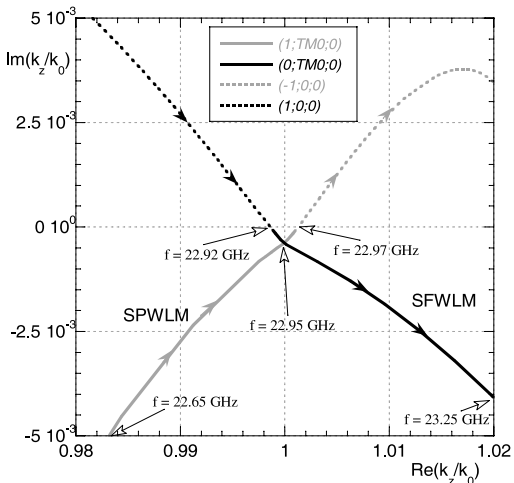

(c)

Figure 4. Pole trajectories in the complex k_z plane for a microstrip as in Figure 2 with three different values of the strip width w: (a) w = 2.9 mm, (b) $w = w_c$ = 3 mm, and (c) w = 3.1 mm. (1; TM_0; 0) pole, gray solid line; (0; TM_0; 0) pole, black solid line; (1; 0; 0) pole, black dotted line; and (−1; 0; 0) pole, gray dotted line.

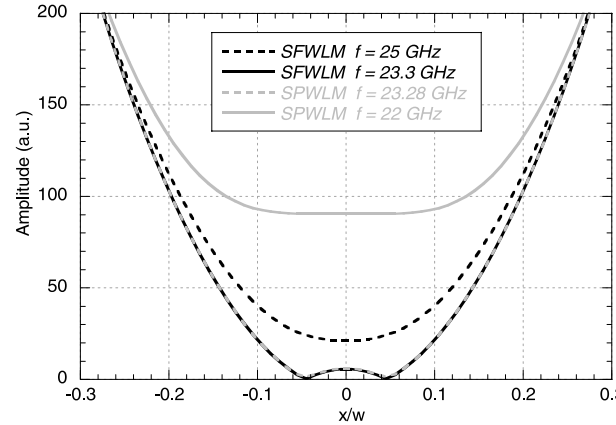

Figure 5. Amplitude of the longitudinal component of the modal current of the SPWLM (f = 22 GHz and f = 23.28 GHz) and of the SFWLM (f = 23.3 GHz and f = 25 GHz) as a function of the normalized transverse coordinate x/w.

ε_r = 2.2, substrate thickness h = 1 mm, and strip width $w = w_c$ = 3.26 mm, which corresponds to the critical strip width for this substrate. Once again a transition from space wave leakage to surface wave leakage can be observed. The choice of a lower dielectric constant for the substrate has the effect of increasing the transition frequency from about 23.29 GHz to about 61.83 GHz; moreover, the critical strip width is now slightly larger than in the previous case.

[22] In Table 1 the normalized critical strip width w_c/h and the normalized transition frequency h/λ_0 corresponding to different values of ε_r are shown. Normalized in this way, the results are valid for any substrate thickness (although the value of h = 1 mm was used in the numerical calculation). For convenience, this table also shows the value of $w_c/\lambda_0 = (w_c/h)(h/\lambda_0)$. The table shows that w_c/h is fairly independent of ε_r, but that h/λ_0 is not, and increases as ε_r decreases. As this table demonstrates, both the substrate thickness and the strip width must be fairly large in terms of a wavelength for a transition to occur. For a substrate permittivity of 10.2, the normalized substrate thickness is 0.077 λ_0 and the strip width is 0.23 λ_0. As the substrate permittivity decreases to a small value of 1.05, these values change to 1.0 λ_0 and 3.3 λ_0, respectively. Hence this transition

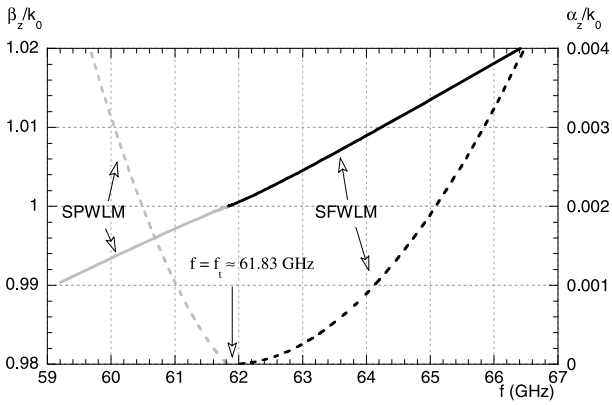

Figure 6. Same as in Figure 3 but for a microstrip with $\varepsilon_r = 2.2$, $h = 1$ mm, and $w = 3.26$ mm.

effect is most likely to be observed at the higher microwave and millimeter wave frequencies, although there does not seem to be any simple quantitative criterion to accurately predict the value of the transition frequency. Also shown in the table is the quasi-static characteristic impedance for each permittivity and critical strip width.

[23] A discussion about the occurrence of a SFWLM-to-SPWLM transition and its relation to the strip width will be presented in the next section.

4. Analysis of the Modal Currents Via the Reciprocity Theorem

[24] In order for a physical SPWLM to evolve into a physical SFWLM, the SPWLM pole trajectory in the k_z plane must evolve according to one of the following two possible scenarios: (1) the pole approaches the branch point at k_0, and after coalescing with the branch point, it re-emerges as a SFWLM solution; that is, it changes sheets on the k_z Riemann surface at the branch point; (2) the pole crosses the Sommerfeld branch cut on the real axis at some point $k_z < k_0$, and at this point it changes sheet. These two cases are considered next. The first one is the actual scenario that is observed, but the second possibility is also considered to illustrate why it is unlikely to ever happen.

Table 1. Normalized Critical Strip Width w_c/h and the Normalized Transition Frequency h/λ_0 for Different Values of the Substrate Relative Permittivity ε_r[a]

Permittivity ε_r	w_c/h	h/λ_0	w_c/λ_0	Z_c, Ω
1.05	3.30	1.00	3.30	64.6
2.2	3.26	0.21	0.67	48.4
4.2	3.15	0.13	0.41	37.2
10.2	3.00	0.077	0.23	25.3

[a]Also included is the value of w_c/λ_0 at the transition frequency and the quasi-static characteristic impedance Z_c for each case.

4.1. Branch Point Crossing

[25] At a transition frequency f_t, we have $k_z = k_0$. For the leaky mode at this frequency, the transverse wave number of the TM_0 mode on the background structure (into which leakage is occurring) is

$$k_x^{TM_0} = \sqrt{k_{TM_0}^2 - k_0^2}. \tag{5}$$

The angle of leakage, θ_0 (see Figure 7a), is given by

$$\tan\theta_0 = \frac{k_x^{TM_0}}{k_z} = \frac{k_x^{TM_0}}{k_0} = \sqrt{\hat{k}_{TM_0}^2 - 1}, \tag{6}$$

where $\hat{k}_{TM_0} = k_{TM_0}/k_0$ and k_{TM_0} is calculated at $f = f_t$. It should be noted that equation (6) is exact when the pole is at the branch point, since $\alpha_z = 0$ at this point.

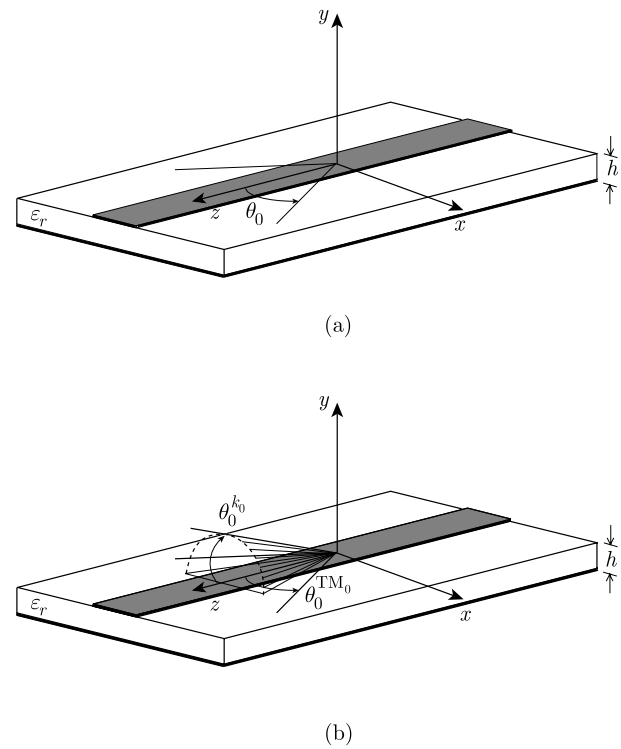

Figure 7. Illustration of the reciprocity theorem applied to the case of a direct SPWLM-SFWLM transition. (a) Branch point crossing (θ_0 is the angle of leakage in the xz plane of the TM_0 surface wave). (b) Branch cut crossing ($\theta_0^{TM_0}$ is the angle of leakage in the xz plane of the TM_0 surface wave and $\theta_0^{k_0}$ is the angle of leakage into space).

[26] Next, it should be enforced that there is no leakage at this frequency, since $\alpha_z = 0$. This means that the current of the leaky mode on the strip (corresponding to a mode on an infinite strip) does not radiate into the TM_0 mode. By reciprocity, this also means that the reaction between the field of a TM_0 mode propagating at the angle θ_0 and the current on the strip will be zero. The tangential electric field (i.e., x and z components) of the TM_0 mode will lie in a direction parallel to the angle of leakage. Hence, assuming for convenience that $x > 0$,

$$\mathbf{E}_t^{\mathrm{TM}_0} = \hat{\mathbf{u}} E_u^{\mathrm{TM}_0}, \tag{7}$$

where

$$\hat{\mathbf{u}} = \left(\hat{\mathbf{x}} k_x^{\mathrm{TM}_0} + \hat{\mathbf{z}} k_z\right)/k_{\mathrm{TM}_0} = \hat{\mathbf{x}} \sin\theta_0 + \hat{\mathbf{z}} \cos\theta_0. \tag{8}$$

[27] By virtue of the reciprocity principle, at the transition frequency f_t, when $k_z = k_0$, we must have (since there is no leakage)

$$\int_{-w/2}^{+w/2} \mathbf{J}_S \cdot \mathbf{E}_t^{\mathrm{TM}_0}\, \mathrm{d}x = 0, \tag{9}$$

where $\mathbf{E}_t^{\mathrm{TM}_0}$ is the tangential component of the field of a TM_0 surface wave mode propagating at an angle θ_0 inward toward the strip (i.e., propagating in the negative x and negative z directions). The above integral in equation (9) can be rewritten as

$$\cos\theta_0 \int_{-w/2}^{+w/2} J_{s,z}(x)\, \mathrm{e}^{jk_x^{\mathrm{TM}_0} x}\, \mathrm{d}x + \sin\theta_0 \int_{-w/2}^{+w/2} J_{s,x}(x)\, \mathrm{e}^{jk_x^{\mathrm{TM}_0} x}\, \mathrm{d}x = 0\ , \tag{10}$$

or, equivalently, as

$$\frac{\tilde{J}_{s,z}\left(k_x^{\mathrm{TM}_0}\right)}{\tilde{J}_{s,x}\left(k_x^{\mathrm{TM}_0}\right)} = -\tan\theta_0, \tag{11}$$

where the tilde indicates Fourier transform with respect to the transverse x variable.

[28] Equation (11) is a necessary condition that would enable a SPWLM to transition into a SFWLM after passing through the branch point at k_0. This result seems to indicate that such a transition is not likely to occur for narrow strips, since the transverse current $\tilde{J}_{s,x}(k_x^{\mathrm{TM}_0})$ on the microstrip line would be in this case very small, and therefore equation (11) could not be satisfied since its right-hand side is not expected to be very large (a further discussion of this is provided in Appendix A). However, for wide strips, where both components of the current can be significant, it is certainly possible, as was shown in section 3.

4.2. Branch Cut Crossing

[29] In this case, there would be a particular frequency for which $k_z = \beta_z < k_0$ (at which the SPWLM pole crosses the branch cut on the real axis in the k_z plane). Following similar reasoning as above, the following condition should then be satisfied:

$$\frac{\tilde{J}_{s,z}\left(k_x^{\mathrm{TM}_0}\right)}{\tilde{J}_{s,x}\left(k_x^{\mathrm{TM}_0}\right)} = -\tan\theta_0^{\mathrm{TM}_0}, \tag{12}$$

where now

$$k_x^{\mathrm{TM}_0} = \sqrt{k_{\mathrm{TM}_0}^2 - {\beta_z}^2} \tag{13}$$

and the angle of surface wave leakage at the substrate interface (see Figure 7b) is

$$\tan\theta_0^{\mathrm{TM}_0} = \frac{k_x^{\mathrm{TM}_0}}{\beta_z}. \tag{14}$$

[30] Moreover, there cannot be leakage into space in any direction, either for TM_z or TE_z waves (since $\alpha_z = 0$), and thus the following two conditions should be also satisfied:

$$\mathrm{TM}: \quad -\sin\theta_0^{k_0} \tilde{J}_{s,z}\left(k_x^0\right) + \cos\theta_0^{k_0} \cos\phi \tilde{J}_{s,x}\left(k_x^0\right) = 0 \tag{15}$$

$$\mathrm{TE}: \quad \sin\phi\, \tilde{J}_{s,x}\left(k_x^0\right) = 0, \tag{16}$$

where

$$k_x^0 = k_0 \sin\theta_0^{k_0} \cos\phi \tag{17}$$

and

$$\cos\theta_0^{k_0} = \frac{\beta_z}{k_0}\ . \tag{18}$$

[31] The angle $\theta_0^{k_0}$ is the angle that the cone of leakage into space makes with respect to the z axis (see Figure 7b). The angle ϕ is the azimuthal rotation angle on the leakage cone, with $\phi = 0$ corresponding to a leakage direction in the xz plane.

[32] Both equations (15) and (16) must be valid for all angles ϕ in order to have no power leakage at any angle ϕ (in other words, at any direction on the leakage cone). Equation (16) implies that $\tilde{J}_{s,x}(k_x) = 0$ over a range of values for k_x ($|k_x| < k_0 \sin\theta_0^{k_0}$). Equation (15) implies that $\tilde{J}_{s,z}(k_x) = 0$ over the same range of k_x. Mathematically,

this cannot happen, at least for any reasonable current distribution. Therefore it is concluded that a transition from a SPWLM to a SFWLM by virtue of the pole trajectory crossing the real axis at a point $\beta_z < k_0$ is not possible (or at least extremely unlikely for any reasonable strip dimensions).

4.3. Validation of the Zero Surface Wave Excitation Condition

[33] In order to verify if the zero surface wave excitation condition of equation (11) for a direct SPWLM-SFWLM transition holds for the cases presented in section 3, we have considered the magnitude of the following quantity:

$$A(f) = \frac{\tilde{J}_{s,z}\left(k_x^{\mathrm{TM}_0}\right)}{\tilde{J}_{s,x}\left(k_x^{\mathrm{TM}_0}\right)} + \tan\theta_0. \tag{19}$$

[34] Equation (11) is satisfied when the quantity $A(f)$ in equation (19) is zero, which is a necessary condition for the SPWLM-SFWLM transition to occur at a frequency $f = f_t$. In Figure 8 we have plotted the magnitude of $A(f)$ in equation (19) versus frequency in a neighborhood of f_t, in order to verify that it does indeed approach zero at $f = f_t$. Results are reported in Figures 8a and 8b for the structures considered in Figures 2 and 6 (high-permittivity and low-permittivity cases, respectively). It can be observed that, as expected, the excitation of the TM_0 surface wave field is zero at the transition frequency f_t in both cases.

[35] In Figure 8c, the $w = w_c = 3$ mm case from Figure 8a is replotted, along with results for a narrower strip (w = 2 mm) and a wider strip (w = 4 mm). This comparison is made in order to demonstrate that the SPWLM-SFWLM transition occurs only for a critical strip width. It is not too surprising that a transition cannot occur for a narrow strip width, since condition (11) requires a significant transverse current, which is increasingly unlikely as the strip width decreases, as explained in more detail in Appendix A. For strip widths that are wider than the critical strip widths shown in Figures 8a and 8b, it is not obvious whether or not additional transitions may occur. The w = 4 mm case shows that a transition frequency does not occur for this wider strip, at least for the frequency range shown. Thus, while it cannot be ruled out that more than one critical strip width may exist, this has not been found for the practical ranges investigated.

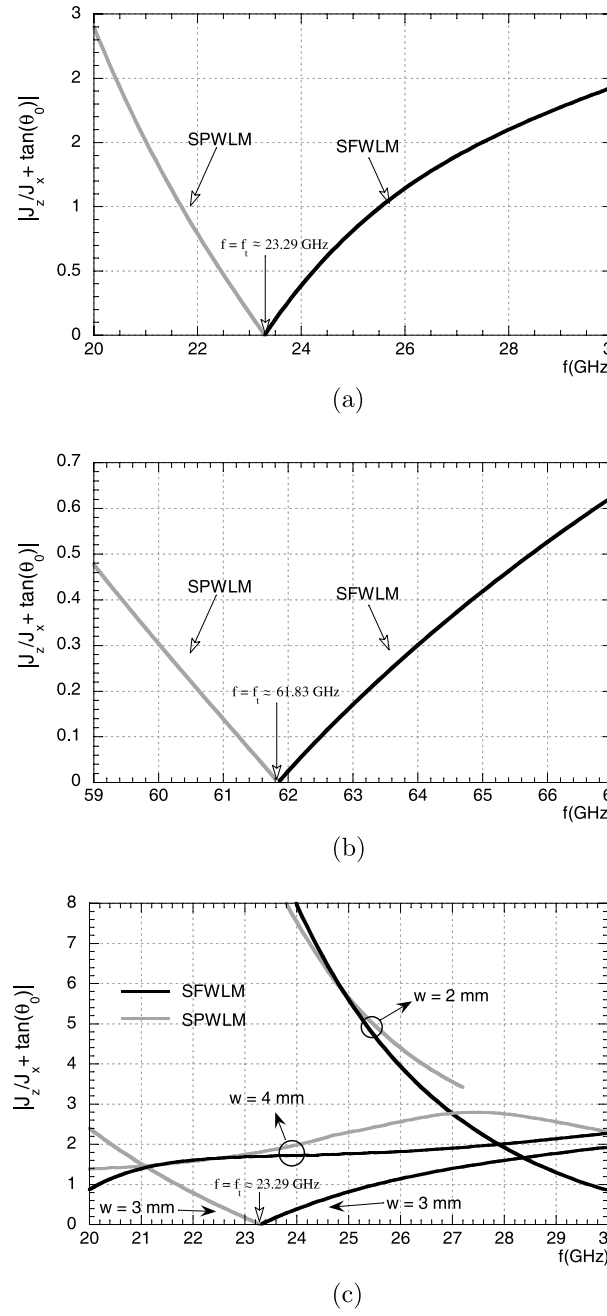

Figure 8. Magnitude of the function $A(f)$, defined in equation (19), versus frequency, which measures the degree of surface wave excitation. (a) Microstrip as in Figure 2. (b) Microstrip as in Figure 6. (c) Same case as in Figure 8a shown together with w = 2 mm and w = 4 mm.

5. Excitation of the Microstrip Line by a Finite Source

[36] The effects of the excitation of either the SPWLM or SFWLM in a neighborhood of the transition frequency have been studied by considering the current excited on

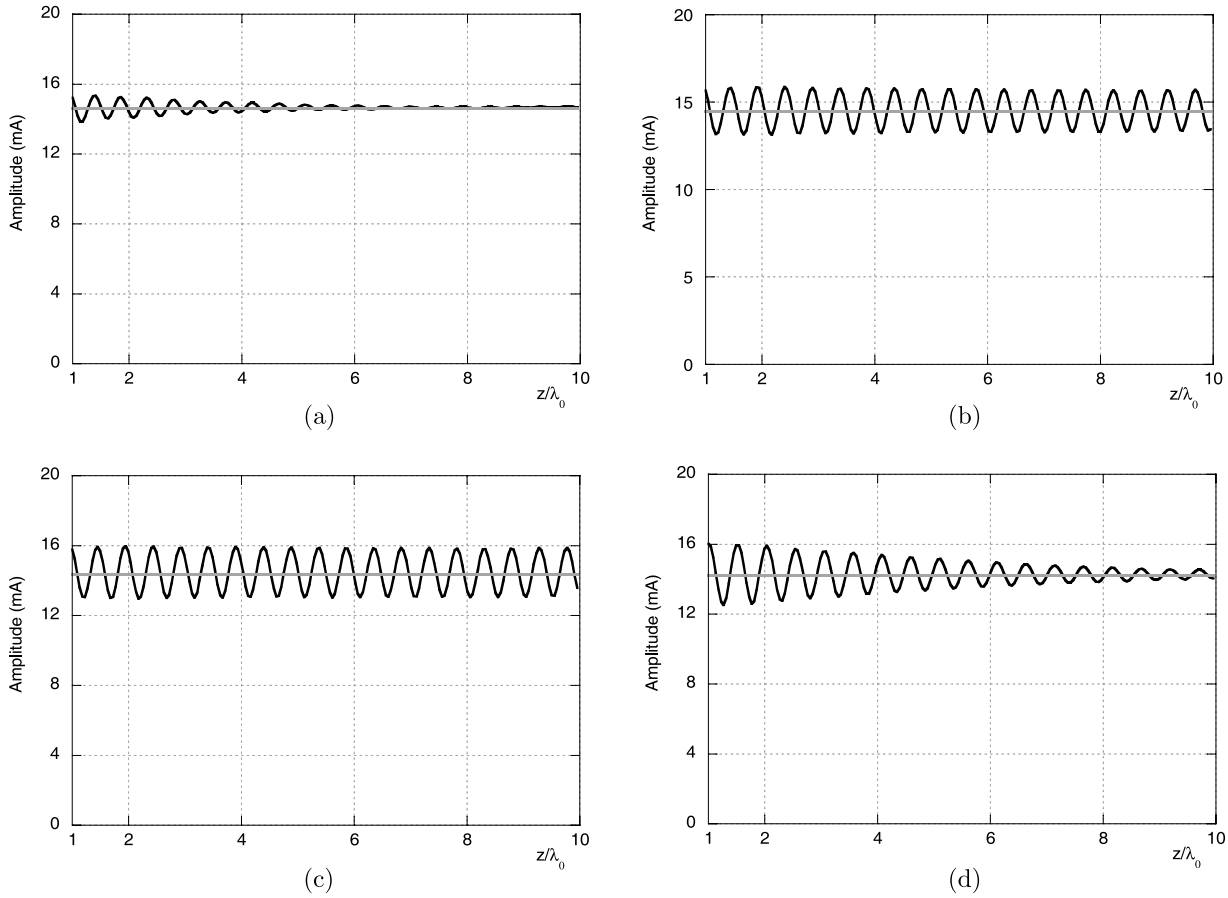

Figure 9. Amplitude of the current excited on an infinitely long microstrip line, with physical parameters as in Figure 2, by a gap voltage source: (a) f = 22 GHz, (b) f = 23.2 GHz, (c) f = 23.5 GHz, and (d) f = 25 GHz. TC, black solid line; BM current, gray solid line.

an infinite microstrip line by a gap voltage source. The analysis has been performed by means of a spectral domain moment-method approach as in the work by *Di Nallo et al.* [1998].

[37] Figure 9 shows the amplitudes of the total current (TC) and BM current as a function of the normalized distance z/λ_0 from the source for a microstrip with parameters as in Figure 2 at different frequencies. The amplitude of the BM current (i.e., the fundamental quasi-TEM EH_0 mode) does not depend on the distance from the source, and it also remains relatively constant with respect to frequency in the considered frequency range. The TC, in contrast, clearly shows large oscillations about the BM current as the distance increases, due to the interference with the CS current. Such oscillations decay with the distance from the source, corresponding to the decay of the CS current. However, such decay tends to disappear as the transition frequency is approached, as evidenced in parts (b) and (c).

[38] In order to clarify the reason for this behavior of the CS current, it is convenient to consider its two essential constituents separately, that is, the LM current (due to either the SPWLM or the SFWLM) and the k_0-RW current (the integral contribution from the vertical SDP through the k_0 branch point). In Figure 10 three frequencies are considered above the transition frequency. Figure 10a shows the CS currents, which are seen to persist to larger distances as the frequency approaches the transition frequency. The CS current is seen to be very well accounted for by the LM currents alone (Figure 10b) since the RW currents are negligible (Figure 10c).

[39] The fact that the decay of the CS current with distance decreases as the transition frequency is approached corresponds to the fact that the attenuation constant of the relevant leaky mode (the SFWLM in

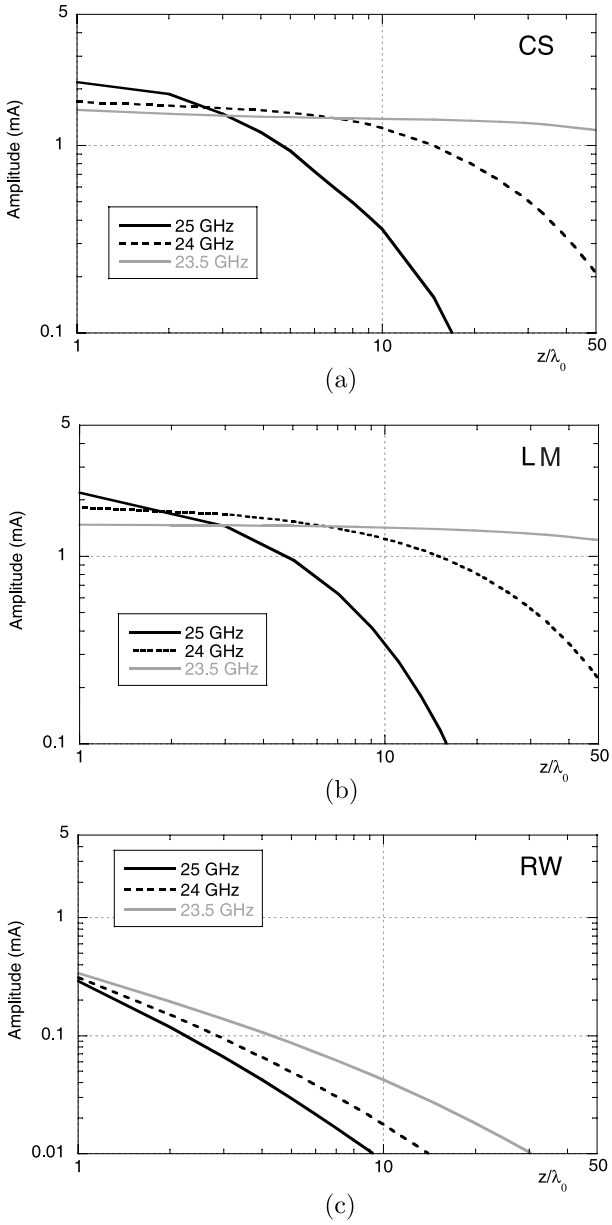

Figure 10. Amplitude of the CS current and its constituent parts as a function of the normalized distance z/λ_0, for the same structure as in Figure 9, at three different frequencies above f_t: (a) CS current, (b) LM current, and (c) k_0-RW current.

Figure 10) tends to zero in this limit. However, considering frequencies above but extremely close to f_t, an interesting phenomenon can be observed, as seen in Figure 11: the LM current decreases in amplitude as f_t is approached, whereas the RW current increases in amplitude, and it also decays more slowly with distance. Thus, for frequencies extremely close to the transition frequency, the RW component accounts almost entirely for the behavior of the CS current.

[40] The same considerations apply for frequencies lower than f_t, where the SPWLM is involved. Figure 12 shows three frequencies that are close (but not extremely close) to f_t, in which the LM current is dominant. In Figure 13 three frequencies extremely close to f_t are

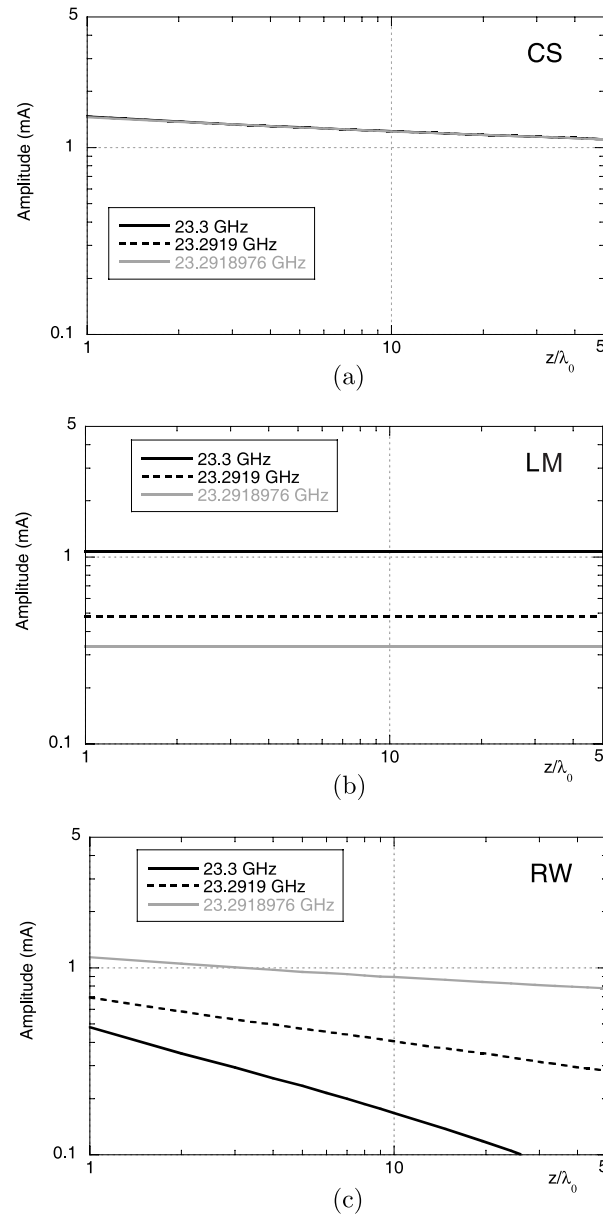

Figure 11. Same as in Figure 10 but at three frequencies extremely close to f_t.

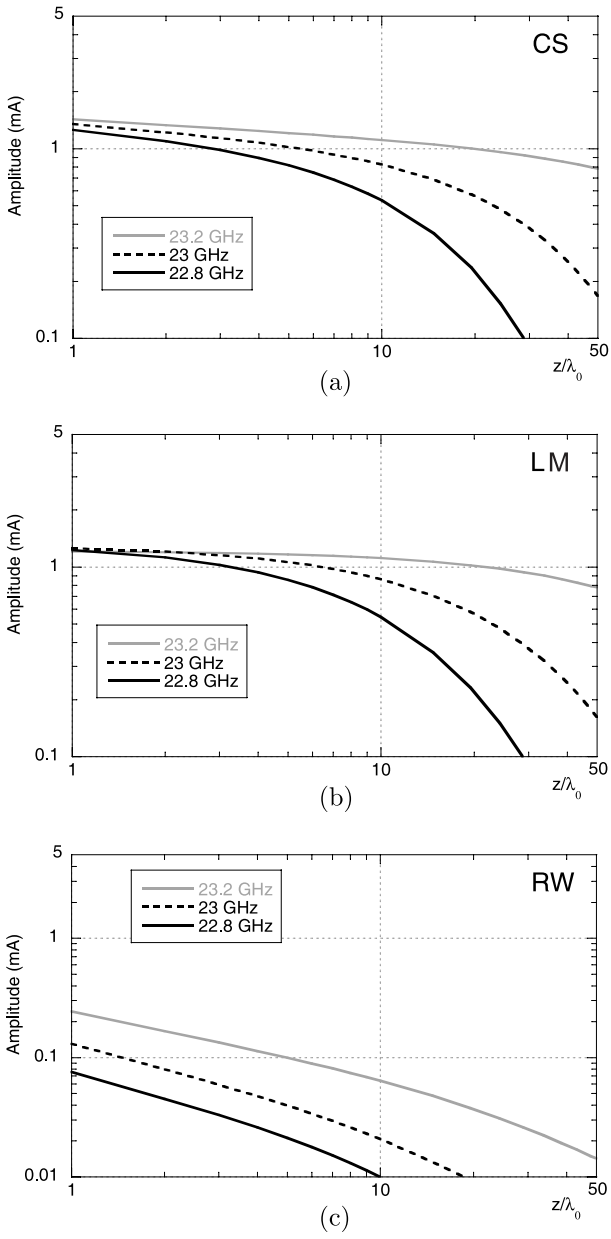

Figure 12. Same as in Figure 10 but at three frequencies below f_t.

reported, where the RW current becomes dominant. From Figures 10–13 it can be concluded that, in a small neighborhood of f_t, the RW current replaces the LM current as the dominant current. This latter fact is confirmed in Figure 14, where the amplitude of the CS current, the k_0-RW current, and the LM current at a fixed distance $z = \lambda_0$ from the source are reported as a function of frequency. It can be clearly observed that while the amplitude of the LM current has a dip at $f = f_t$, the k_0-RW current has a local maximum, such that their sum produces a CS current that varies smoothly with frequency.

[41] To explore the nature of the RW current near the transition frequency from a more mathematical perspective, Figure 15 shows a plot of the magnitude

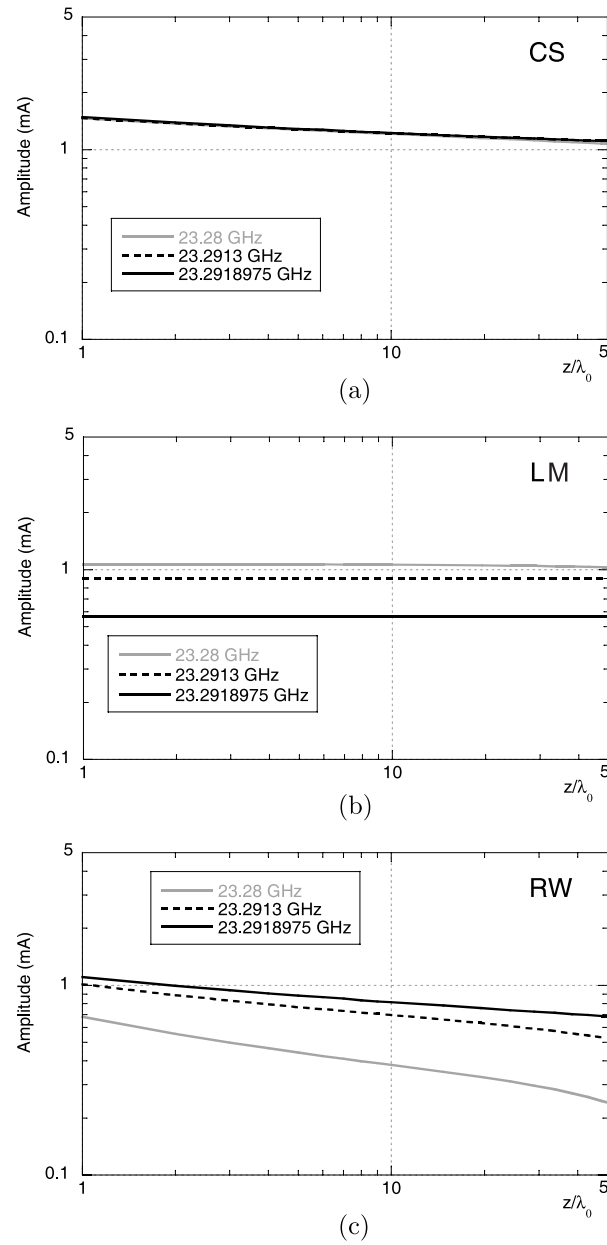

Figure 13. Same as in Figure 12 but at three frequencies below and extremely close to f_t.

of the $F(s)$ function (see equation (3)) versus s (the distance along the SDP from the k_0 branch point) for various frequencies close to the transition frequency. For frequencies that are not too close, the $F(s)$ function exhibits a behavior of s (i.e., a linear function) for small s [*Baccarelli et al.*, 2004]. As shown by *Jackson et al.* [2000] and *Baccarelli et al.* [2004], Watson's lemma directly relates the asymptotic behavior of the $F(s)$ function near $s = 0$ with the asymptotic behavior of the RW current for large z. In particular, the linear behavior of the $F(s)$ function corresponds with a RW current that behaves asymptotically as $1/z^2$ [*Mesa et al.*, 2001; *Baccarelli et al.*, 2004]. This is the usual expected asymptotic behavior of the k_0-RW current on a microstrip line [*Mesa et al.*, 2001; *Baccarelli et al.*, 2004].

[42] However, as the frequency approaches near to the transition frequency, the behavior of the $F(s)$ function begins to change. For frequencies close to the transition frequency, the $F(s)$ function exhibits a growing behavior, similar to (but not exactly equal to) a $1/s$ behavior. This in turn implies that the behavior of the RW current with distance z is very different, and in particular, much more slowly decaying, than a $1/z^2$ behavior. However, extremely close to the branch point (i.e., for extremely small s), the $F(s)$ function always changes its behavior and assumes a linear variation. This transition region, where the $F(s)$ function changes nature, occurs for smaller s as the frequency gets closer to the transition frequency. This implies that for frequencies that are extremely close to the transition frequency, the RW current will decay very slowly out to an extremely large distance before the behavior finally changes to a $1/z^2$ behavior. This slowly decaying behavior is evident in Figures 11c and 13c at the frequencies of 23.2918976 and 23.2918975 GHz, respectively (the transition region in z where the RW current changes to a $1/z^2$ behavior is very large and is off the scale of these plots.)

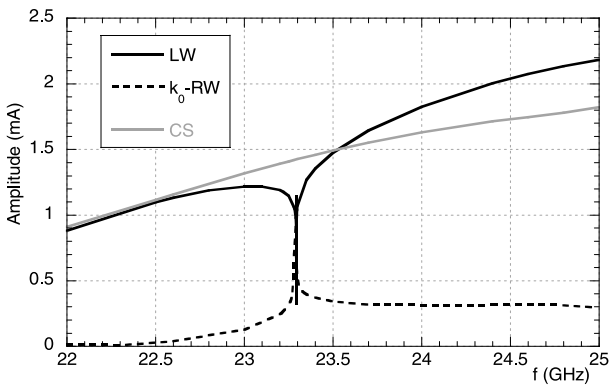

Figure 14. Amplitude of the CS current, the LW current, and the k_0-RW current, at a fixed distance $z = \lambda_0$ from the source, for the same structure as in Figures 9–13, as a function of frequency.

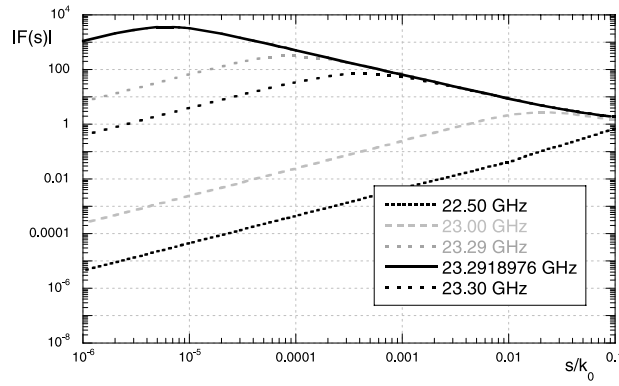

Figure 15. Plot of the magnitude of the $F(s)$ function versus the normalized distance s/k_0 along the SDP from the k_0 branch point, for the same structure as in Figures 9–13.

6. Conclusion

[43] In this paper examples have been reported of a new modal transition between surface wave and space wave leaky modes on a microstrip line. This transition occurs at a particular transition frequency when the strip has a critical strip width, which is fairly wide. This transition has been explained by means of the reciprocity theorem, showing that at the transition frequency the leaky mode current on the line does not radiate into the surface wave. The analysis has also revealed that such a direct transition is only likely to occur on microstrip lines with a wide strip.

[44] By considering a microstrip line excited by a gap voltage source, it has been shown that interference between the continuous spectrum current and the bound mode current may give rise to noticeable spurious effects close to the transition frequency. An analysis of the continuous spectrum current has shown that it is dominated by a physical leaky mode current for frequencies that are near, but not too near, the transition frequency. In a very small frequency range around the transition frequency, the leaky mode is weakly excited and the residual wave current assumes the dominant role in determining the continuous spectrum current, and hence in explaining the interference effects.

Appendix A: Discussion of the Transition Condition for Small Width

[45] The transition equation (11) is a necessary condition for the SPWLM-SFWLM transition to occur. Fur-

ther physical insight can be gained by studying the left-hand side of this equation in the limit of a small strip width.

[46] Consider first the Fourier transform of the z component of the current,

$$\tilde{J}_{s,z}(k_x) = \int_{-w/2}^{w/2} J_{s,z}(x)\, e^{jk_x x}\, dx = 2\int_0^{w/2} J_{s,z}(x)\, \cos(k_x x)\, dx\,, \tag{A1}$$

where $J_{s,z}(x)$ has been assumed to be an even function of x. Next, a normalized shape function $N_z(\bar{x})$, defined on the interval $\bar{x} \in (0, 1)$, is introduced to account for the shape of the $J_{s,z}(x)$ function. This normalized function can be roughly viewed as a basis function for the z component of current (if this function is allowed to change with frequency and w, then no approximation is being made). By writing

$$J_{s,z}(x) = A_z\, N_z(\bar{x}) \tag{A2}$$

and using the substitution $\bar{x} = (2/w)x$, we have

$$\tilde{J}_{s,z}(k_x) = wA_z \int_0^1 N_z(\bar{x})\, \cos\left[\left(k_x \frac{w}{2}\right)\bar{x}\right] d\bar{x} = wA_z \tilde{N}_z^{\cos}\left(k_x \frac{w}{2}\right)\,, \tag{A3}$$

where $\tilde{N}_z^{\cos}(\xi)$ is the cosine-Fourier transform of $N_z(\bar{x})$. For the x component of the current, we can follow a similar procedure by expressing

$$J_{s,x}(x) = A_x\, N_x(\bar{x})\,. \tag{A4}$$

[47] Since this current component is an odd function, we can write

$$\tilde{J}_{s,x}(k_x) = jwA_x \tilde{N}_x^{\sin}\left(k_x \frac{w}{2}\right), \tag{A5}$$

where $\tilde{N}_x^{\sin}(\xi)$ is the sine-Fourier transform of $N_x(\bar{x})$. Note that as ξ (and hence w) becomes small, the sine transform tends to zero. Hence it is useful to write

$$\tilde{N}_x^{\sin}(\xi) = \xi \int_0^1 \bar{x}\, N_x(\bar{x})\, \mathrm{sinc}(\xi\bar{x})\, d\bar{x}\,. \tag{A6}$$

[48] Let us define the sinc transform of N_x as

$$\tilde{N}_x^{\mathrm{sinc}}(\xi) = \int_0^1 \bar{x}\, N_x(\bar{x})\, \mathrm{sinc}(\xi\bar{x})\, d\bar{x} \tag{A7}$$

so that

$$\tilde{N}_x^{\sin}(\xi) = \xi\, \tilde{N}_x^{\mathrm{sinc}}(\xi)\,. \tag{A8}$$

[49] The transition condition in equation (11) can be then expressed as

$$\left(\frac{A_x}{A_z}\right)\left(k_x^{\mathrm{TM}_0} w\right)\left[\frac{\tilde{N}_x^{\mathrm{sinc}}\left(k_x^{\mathrm{TM}_0} w/2\right)}{\tilde{N}_z^{\cos}\left(k_x^{\mathrm{TM}_0} w/2\right)}\right] = j\cot\theta_0. \tag{A9}$$

[50] Note that in this normalized expression, the main effect of varying the strip width w has been taken outside the integral, and put into the product $k_x^{\mathrm{TM}_0} w$. Certainly, the ratio of the normalized transforms (the rightmost fraction on the left-hand side of equation (A9)) varies with w, since the shapes of the normalized currents will vary somewhat with w. However, this variation should not be too large, and in fact, this latter ratio should approach a constant as w becomes small. Therefore equation (A9) implies that the transition can only occur when

$$\left(\frac{A_x}{A_z}\right) k_0\, w = \mathcal{O}(1). \tag{A10}$$

[51] Equation (A9) gives some physical insight into how wide the strip has to be for the SPWLM-SFWLM transition to occur. It is shown below that the ratio A_x/A_z approaches zero as $k_0 w$ becomes small, at least as fast as the product $k_0 w$. Hence the left-hand side of equation (A9) becomes small at least as fast as $(k_0 w)^2$. Therefore it is extremely difficult for a SPWLM-SFWLM transition to occur for narrow strips.

[52] Next we explore how the ratio A_x/A_z depends on w, for small w. The surface divergence condition implies that the current components are related to the charge density ρ_s on the strip as

$$\frac{\partial J_{s,x}}{\partial x} + \frac{\partial J_{s,z}}{\partial z} = -j\,\omega\,\rho_s. \tag{A11}$$

[53] (In this equation the charge density ρ_s is actually the sum of the charge densities on both sides of the strip.) Equation (A11) can be written as

$$A_x\left(\frac{2}{w}\right)\frac{\partial N_x(\bar{x})}{\partial \bar{x}} - j\,k_z\,A_z\,N_z(\bar{x}) = -j\,\omega\,\rho_s. \tag{A12}$$

[54] The propagation wave number can be written as $k_z = k_0\sqrt{\varepsilon_r^{\mathrm{eff}}}$, and it is concluded that

$$j\left(\frac{2}{w}\right)\left(\frac{A_x}{A_z}\right)\frac{\partial N_x(\bar{x})}{\partial \bar{x}} = \frac{\omega\,\rho_s}{A_z} - k_0\,N_z(\bar{x})\sqrt{\varepsilon_r^{\mathrm{eff}}} \tag{A13}$$

or, equivalently,

$$\left(\frac{A_x}{A_z}\right) = \left(\frac{k_0\, w}{2}\right)\left(\frac{-jN_z(\bar{x})}{N_x'(\bar{x})}\right)\left[\frac{c\,\rho_s}{J_{s,z}} - \sqrt{\varepsilon_r^{\text{eff}}}\right], \quad \text{(A14)}$$

where c is the speed of light. The term within the square brackets is exactly zero if the mode is a TEM mode. For a quasi-TEM leaky mode, we can make the assumption that the current density on the strip becomes more TEM-like as w becomes smaller. In this case, the above term approaches zero as w becomes small. Hence the ratio A_x/A_z must approach zero as w approaches zero even faster than $k_0 w$ for a quasi-TEM leaky mode, as claimed above.

[55] **Acknowledgment.** The work of F. Mesa was partially supported by Spanish Ministerio de Educación y Ciencia under project TEC2004-03214 and by Junta de Andalucía. The work of D. R. Jackson was partially supported by the State of Texas Advanced Technology Program.

References

Baccarelli, P., P. Burghignoli, F. Frezza, A. Galli, G. Lovat, and S. Paulotto (2004), Asymptotic analysis of bound-mode and free-space residual-wave currents excited by a delta-gap source on a microstrip line, *Radio Sci.*, *39*, RS3011, doi:10.1029/2003RS002918.

Bagby, J. S., C.-H. Lee, D. P. Nyquist, and Y. Yuan (1993), Identification of propagation regimes on integrated microstrip transmission lines, *IEEE Trans. Microwave Theory Tech.*, *41*, 1887–1893.

Chang, D. C., and E. F. Kuester (1979), An analytic theory for narrow open microstrip, *Arch. Elek. Uebertraeg.*, *33*, 199–206.

Das, N. K., and D. M. Pozar (1991), Full-wave spectral-domain computation of material, radiation, and guided wave losses in infinite multilayered printed transmission lines, *IEEE Trans. Microwave Theory Tech.*, *39*, 54–63.

Di Nallo, C., F. Mesa, and D. R. Jackson (1998), Excitation of leaky modes on multilayer stripline structures, *IEEE Trans. Microwave Theory Tech.*, *46*, 1062–1071.

Freire, M. J., F. Mesa, C. Di Nallo, D. R. Jackson, and A. A. Oliner (1999), Spurious transmission effects due to the excitation of the bound mode and the continuous spectrum on stripline with an air gap, *IEEE Trans. Microwave Theory Tech.*, *47*, 2493–2502.

Grimm, J. M., and D. P. Nyquist (1993), Spectral analysis considerations relevant to radiation and leaky modes of open-boundary microstrip transmission line, *IEEE Trans. Microwave Theory Tech.*, *41*, 150–153.

Jackson, D. R., F. Mesa, M. J. Freire, D. P. Nyquist, and C. D. Nallo (2000), An excitation theory for bound modes, leaky modes, and residual-wave currents on stripline structures, *Radio Sci.*, *35*, 495–510.

Langston, W. L., J. T. Williams, D. R. Jackson, and F. Mesa (2001), Spurious radiation from a practical source on a covered microstrip line, *IEEE Trans. Microwave Theory Tech.*, *49*, 2216–2226.

Mesa, F., and D. R. Jackson (2002a), The danger of high-frequency spurious effects on wide microstrip line, *IEEE Trans. Microwave Theory Tech.*, *50*, 2679–2690.

Mesa, F., and D. R. Jackson (2002b), Investigation of integration paths in the spectral-domain analysis of leaky modes on printed circuit lines, *IEEE Trans. Microwave Theory Tech.*, *50*, 2267–2275.

Mesa, F., C. Di Nallo, and D. R. Jackson (1999), The theory of surface-wave and space-wave leaky-mode excitation on microstrip lines, *IEEE Trans. Microwave Theory Tech.*, *47*, 207–215.

Mesa, F., D. R. Jackson, and M. J. Freire (2001), High-frequency leaky-mode excitation on a microstrip line, *IEEE Trans. Microwave Theory Tech.*, *49*, 2206–2215.

Mesa, F., D. R. Jackson, and M. J. Freire (2002), Evolution of leaky modes on printed-circuit lines, *IEEE Trans. Microwave Theory Tech.*, *50*, 94–104.

Oliner, A. A. (1987), Leakage from higher modes on microstrip lines with application to antennas, *Radio Sci.*, *22*, 902–912.

Rodríguez-Berral, R., F. Mesa, and F. Medina (2004), Two-dimensional study of leaky modes in microstrip lines with a semi-infinite cover layer, *Radio Sci.*, *39*, RS4002, doi:10.1029/2003RS003007.

Shigesawa, H., M. Tsuji, and A. A. Oliner (1988), Conductor-backed slot line and coplanar waveguide: Dangers and full-wave analysis, in *1988 IEEE MTT International Microwave Symposium Digest*, vol. 1, pp. 199–202, IEEE Press, Piscataway, N. J.

P. Baccarelli, P. Burghignoli, and S. Paulotto, Department of Electronic Engineering, "La Sapienza" University of Rome, I-00184 Rome, Italy. (baccarelli@die.uniroma1.it)

D. R. Jackson, Department of Electrical and Computer Engineering, University of Houston, Houston, TX 77204-4005, USA.

G. Lovat, Department of Electrical Engineering, "La Sapienza" University of Rome, I-00184 Rome, Italy.

F. Mesa, Department of Applied Physics 1, University of Seville, E-41012 Seville, Spain.